Journal of Neurochemistry, 2007, **102**, 789–800 doi:10.1111/j.1471-4159.2007.04564.x

Excitotoxicity-related endocytosis in cortical neurons

A. Vaslin, J. Puyal, T. Borsello and P. G. H. Clarke

Département de Biologie Cellulaire et de Morphologie, University of Lausanne, Switzerland

Abstract

Recent studies showed that endocytosis is enhanced in neurons exposed to an excitototoxic stimulus. We here confirm and analyze this new phenomenon using dissociated cortical neuronal cultures. NMDA-induced uptake (FITC-dextran or FITC or horseradish peroxidase) occurs in these cultures and is due to endocytosis, not to cell entry through damaged membranes; it requires an excitotoxic dose of NMDA and is dependent on extracellular calcium, but occurs early, while the neuron is still intact and viable. It involves two components, NMDA-induced and constitutive, with different characteristics. Neither component involves specific binding of the endocytosed molecules to a saturable receptor. Strikingly, molecules internalized by the NMDA-induced component are targeted to neuronal nuclei. This component, but not the constitutive one, is blocked by a c-*Jun* N-terminal protein kinase inhibitor. In conclusion, an excitotoxic dose of NMDA triggers c-*Jun* N-terminal protein kinase-dependent endocytosis in cortical neuronal cultures, providing an *in vitro* model of the excitotoxicity-induced endocytosis reported in intact tissues.

Keywords: c-*Jun* N-terminal kinase, dextran, D-JNKI1, neurons, NMDA, primary culture.

J. Neurochem. (2007) **102**, 789–800.

Endocytosis is the main mechanism by which cells internalize material from their extracellular environment, and has the additional roles of down-regulating the membrane expression of certain molecules, notably receptors, and adjusting the total amount of plasma membrane following exocytosis. From the initial membrane-derived vesicles, the endocytosed molecules can be recycled to the plasma membrane or transported to various destinations including lysosomes (Conner and Schmid 2003). It plays a crucial role in many cellular events such as homeostasis, signal transduction, neurotransmission, and the immune response (Sorkin and von Zastrow 2002; Conner and Schmid 2003). Many forms of endocytosis, including receptor-mediated endocytosis and compensatory endocytosis following exocytosis, depend on the formation of clathrin-coated vesicles (Jarousse and Kelly 2001). Other forms are largely independent of clathrin, but are mediated by cholesterol-rich membrane domains such as lipid rafts and caveolae, or by still other routes that are poorly understood (Kirkham and Parton 2005).

The present study focuses on endocytosis in the context of neuronal excitotoxicity. In most cases excitotoxic cell death results from calcium overload, the activation of calcium-dependent enzymes, and mitochondrial dysfunction (Arundine and Tymianski 2003). Excitotoxicity is involved in many neurological conditions, including cerebral ischemia and traumatic brain injury, and appears to play an important role in most neurodegenerative diseases (Doble 1999; Aarts *et al.* 2003). Endocytosis is enhanced in at least two cases of excitotoxicity: retinal amacrine cells of chick embryos following an intraocular injection of kainate (KA) (Borsello *et al.* 2003a), and pyramidal neurons in organotypic hippocampal cultures exposed to a toxic dose of *N*-methyl D-aspartate (NMDA) (Borsello *et al.* 2003c).

The pathways mediating excitotoxic cell death are complex, but in many cases involve the activation of mitogen-activated protein kinases (Borsello *et al.* 2003b; Waxman and Lynch 2005) which are also involved in mediating certain forms of endocytosis (Cavalli *et al.* 2001; Borsello *et al.* 2003c; Pelkmans *et al.* 2005). D-JNKI1, a cell-penetrating and protease-resistant peptide selectively inhibiting the interaction of c-*Jun* N-terminal protein kinase (JNK) with

Received October 24, 2006; revised manuscript received January 17, 2007; accepted February 14, 2007.

Address correspondence and reprint requests to Anne Vaslin, Département de Biologie Cellulaire et de Morphologie (DBCM), University of Lausanne, Rue du Bugnon 9, CH-1005 Lausanne, Switzerland. E-mail: anne.vaslin@unil.ch

Abbreviations used: AF488, AlexaFluor 488; FD150, 150 kDa FITC-dextran; FD4, 4.4 kDa FITC-dextran; FITC, fluorescein isothiocyanate; GLU, glutamate; HRP, horseradish peroxidase; JNK, c-*Jun* N-terminal protein kinase; KA, kainate; LDH, lactate dehydrogenase; MK-801, (5*S*, 10*R*)-(-)-5-methyl-10,11-dihydro-5H-dibenzo[a,d]cyclohepten-5,10-imine hydrogen maleate; NMDA, *N*-methyl D-aspartate; PBS, phosphate-buffered saline; PI, propidium iodide; TMB, tetramethylbenzidine.

many of its targets was previously shown to block NMDA-induced endocytosis of horseradish peroxidase (HRP) by pyramidal neurons in organotypic hippocampal slices (Borsello *et al.* 2003c) as well as protecting the neurons from death.

To examine the mechanisms inducing excitotoxicity-associated endocytosis, and to clarify its involvement in the mediation of neuronal death, we have developed an *in vitro* model relying on the NMDA-induced uptake of fluorescein isothiocyanate (FITC)-labeled dextran by dissociated cortical neurons. In the present paper we confirm that the uptake is by endocytosis rather than leakage through damaged membranes, and describe a method for quantifying it. Using this method, we characterize the phenomenon, showing that the neurons undergo both constitutive endocytosis and NMDA-induced endocytosis. These two types of endocytosis are distinct in that the NMDA-induced component is sensitive to the size of the FITC-labeled dextran and dependent on the c-*Jun* N-terminal kinase pathway, whereas the constitutive component is independent of both.

Materials and methods

Chemicals

N-methyl D-aspartate, free FITC, FITC-dextrans, and HRP were obtained from Sigma-Aldrich Co., (St. Louis, MO, USA). Alexa-Fluor488-dextran was obtained from Invitrogen (Carlsbad, CA, USA). Glutamate (GLU) and (5*S*,10*R*)-(-)-5-methyl-10, 11-dihydro-5H-dibenzo[a,d]cyclohepten-5,10-imine hydrogen maleate (MK-801) were from Tocris, kainic acid (kainate) from Opika.

Primary cell culture

Primary neuronal cultures of cerebral cortex were prepared from 2-day-old Sprague–Dawley rats. Briefly, small pieces of cortex were dissected and incubated with 200 units of papaïn for 30 min at 34°C. For biochemical analysis, dissociated cells were plated at densities of approximately 0.6×10^6 cells/dish on poly-D-lysine pre-coated 35 mm dishes in B27/Neurobasal (Invitrogen) supplemented with 0.5 mmol/L glutamine and 100 μg/mL penicillin–streptomycin. Cells were maintained at 37°C with a 5% CO_2-containing atmosphere for 12 days, with half of the media changed every 3–4 days. Morphological studies were done using 12 mm pre-coated coverslips plated at a density of approximately 15×10^5 cells/dish.

Assay for FITC uptake and quantification of cell death

Cells were incubated in the presence or absence of various doses of NMDA (30, 60, or 100 μmol/L) for 1 or 6 h, and were exposed for an equal time (1 or 6 h) to FITC-dextran (4.4 kDa, 0.5 mg/mL) or free FITC (1.25 μg/mL). Dishes were then placed on ice and rinsed five times with cold phosphate-buffered saline (PBS)-$MgCl_2$ for 5 min. Cells were lysed using 200 μL of lysis buffer (20 mmol/L HEPES, pH 7.4; 10 mmol/L NaCl; 3 mmol/L $MgCl_2$; 2.5 mmol/L EGTA; 0.1 mmol/L dithiothreitol; 50 mmol/L NaF; 1 mmol/L Na_3VO_4; and 1% Nonidet-P40) for 10 min on ice and were then harvested. Cells from three dishes were pooled together and centrifuged in lysis buffer at 4°C for 10 min at 335 *g* to remove cellular debris. The fluorescence of the supernatant was measured at excitation wavelength 494 nm and emission 518 nm. Three dishes were pooled for each measurement and each measurement was repeated in at least three different experiments. Measurements were normalized with respect to the non-NMDA control mean value for each set of experiments.

Cell death was assayed by measurement of lactate dehydrogenase (LDH) released in the medium using the Cytotox 96 non-radioactive cytotoxicity assay kit (Promega, Madison, WI, USA). Absorbance measurements (representing LDH concentration) were converted into percentage of neuronal death values by dividing by the average absorbance for total LDH (from medium plus lysed neurons), measured in different dishes but from same culture.

Propidium iodide (PI) is a polar compound which only enters cells with damaged cell membranes. It binds to nucleic acids and becomes brightly red fluorescent. The dye is said to be non-toxic to neurons and is widely used as a positive indicator of neuronal damage and cell death (Noraberg *et al.* 1999). For morphological studies, cells were exposed to 5 μg/mL PI (Sigma) in PBS–$MgCl_2$ for 5 min on ice and then washed three more times with cold PBS–$MgCl_2$.

Tetramethylbenzidine assay for peroxidase uptake

The uptake of HRP was measured in experiments similar to those for monitoring FITC-dextran uptake, but performed in the presence of 0.5 mg/mL HRP. Cellular HRP activity was measured using 3,3′,5,5′-tetramethylbenzidine (TMB) as HRP substrate. Briefly TMB was dissolved in phosphate citrate buffer containing H_20_2 at 0.6%. 100 μL of sample was incubated with TMB substrate for 3 min. The reaction was stopped by adding 0.5 mol/L H_2SO_4, and the absorbance of the reaction product was read at 405 nm. Measurements were normalized with respect to the non-NMDA control value, which was arbitrarily set to 100%.

Peptidic JNK inhibitor

The JNK-inhibitory peptide D-JNKI1 is a retro-inverso analog (D-amino acids in reversed sequence) of L-JNKI1, which contains a 20-aa sequence of the JNK binding domain of Islet-Brain-1/JNK-interacting protein-1 scaffold protein, linked to the 10-aa intracellular delivery vector trans-activator of transcription $(TAT)_{48–57}$ from the HIV TAT protein (Borsello *et al.* 2003b). The use of a retro-inverso analog provides resistance to degradation by proteases while conserving, at least approximately, the original tertiary structure. D-JNKI1 does not inhibit the activity of c-*Jun* N-terminal kinase (JNK), but blocks its interaction with those of its targets that contain a JNK-binding domain (Bonny *et al.* 2005). In all experiments 2 μmol/L D-JNKI1 was added 1 h before NMDA treatment, which gives strong protection against excitotoxicity (Borsello *et al.* 2003b).

Time-lapse microscopy

Neurons were grown in a time-lapse chamber for 12 days and then exposed to 0.5 mg/mL AlexaFluor488-dextran (AF488-dextran) for 25 min in presence or absence of 100 μmol/L NMDA. Cells were then washed two times with complete medium. To permit high-resolution imaging with an inverted microscope, we plated neurons onto HCl-cleaned, poly-D-lysine-coated glass coverslips (Carolina Biologicals, Burlington, NC, USA) that had previously been

attached using hot vaseline/wax (50 : 50) to 35 mm plastic culture dishes (Corning, Lowell, MA, USA) in which holes 15 mm in diameter had been machine drilled (Lebrand *et al.* 2004). After 12 days in culture, the lids were removed and the dishes placed on the stage of a Nikon TE300 microscope. Temperature was maintained at 37°C and CO_2 was maintained at 5% using a microscope incubator system (Solent Scientific Limited, Segensworth, UK). Selected neurons were imaged with a 20 × /0.95NA planar Apo objective at 20 min intervals. Images were captured with an Orca-ER cooled CCD camera (Hamamatsu, Japan). All peripherals were controlled with Metamorph software (Universal Imaging, Downington, PA, USA). Images were processed in Adobe Photoshop or Metamorph.

Immunofluorescent imaging

Cells were washed three times with PBS–$MgCl_2$ on ice and mounted in Fluorsave mounting medium (Calbiochem, San Diego, CA, USA). Several artifactual localizations of various compounds after different fixation procedures have already been observed (Richard *et al.* 2003), depending on the size or on the charge composition of the product. Cells were therefore not fixed and were examined in the 2 days following experiment. Confocal imaging was performed on a LSM 510 Meta confocal microscope (Carl Zeiss, Thornwood, NY, USA). Images were processed with LSM 510 software and mounted using Adobe Photoshop.

Statistical analysis

Data were analyzed statistically by one-way ANOVA followed by Students' *t*-test (one-tailed, two-sample, and unequal variance).

Results

NMDA-enhanced uptake of FITC-dextran is concentration- and time-dependent

Increasing doses of NMDA (30 μmol/L, 60 μmol/L, or 100 μmol/L) were applied for either 1 or 6 h on the cultured neurons. Control neurons were not exposed to NMDA, permitting the quantification of constitutive uptake. The results in Fig. 1a show that the constitutive uptake of 4, 4-kDa FITC-dextran increased with the duration of incubation and that NMDA stimulation enhanced the uptake. The induced increase depended on both the exposure time (111% increase after 1 h of 100 μmol/L NMDA and 235% after 6 h of NMDA) and the NMDA concentration: the slight increase induced by 30 μmol/L NMDA was not significant after 1 or 6 h of NMDA exposure, whereas 60 and 100 μmol/L NMDA induced significant increases at both observed times. A standard dose of 100 μmol/L NMDA was chosen for all subsequent experiments as it induced the greatest enhancement in endocytosis.

The effect of NMDA on cell death was assessed by measuring LDH release in the medium (Fig. 1b). One hour of 100 μmol/L NMDA stimulation induced little if any neuronal death (5.8%) whereas 6 h of NMDA exposure at the same concentration evoked a very consistent cell death

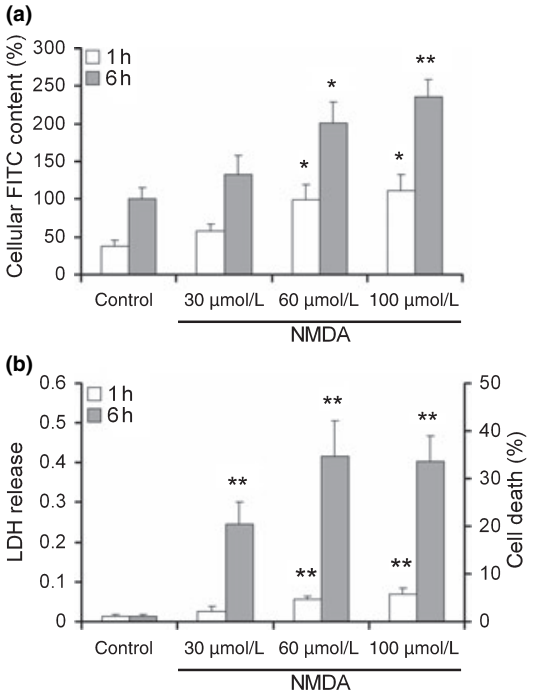

Fig. 1 Dose- and time-dependent effects of *N*-methyl D-aspartate (NMDA) on fluorescein isothiocyanate (FITC)-dextran uptake and cell death. (a) Uptake of 4.4-kDa FITC-dextran after either 1 or 6 h of NMDA exposure ($n = 3$, with three dishes pooled for each measure). Results have been normalized with respect to the 6 h control. ANOVA showed significant differences between the 1 h groups ($p = 0.033$) and between the 6 h groups ($p = 0.013$). Comparisons with the corresponding control: $^{*}p < 0.05$, $^{**}p < 0.01$ (*t*-test). (b) Cell death in the same cultures, assessed from lactate dehydrogenase (LDH) release in the medium. Results are expressed as the difference of LDH after and before the experiment and have been normalized with respect to the control (without NMDA) value ($n = 3$). ANOVA showed significant differences between the 1 h groups ($p = 0.0018$) and between the 6 h groups ($p = 0.0002$). Comparisons with the corresponding control: $^{**}p < 0.01$ (*t*-test). Error bars represent SEM.

(33.6%). After 1 h of 30 μmol/L NMDA, even though there was almost no cell death (2.1%), a slight increase (x1.5) in FITC-dextran endocytosis occurred, but not significant. The fact that the threshold NMDA concentrations for induced endocytosis and for cell death were similar suggests a link between NMDA-induced endocytosis and cell death that remains to be elucidated.

The NMDA-evoked cellular FITC-dextran uptake is energy dependent

To evaluate whether the dextran uptake was due to a physiological temperature sensitive process such as endocytosis, we tested if incubation on ice blocked it. Cells were pre-incubated on ice for 30 min and were then exposed to 100 μmol/L NMDA for 1 h, still on ice. FITC-dextran incorporation was greatly decreased by the temperature

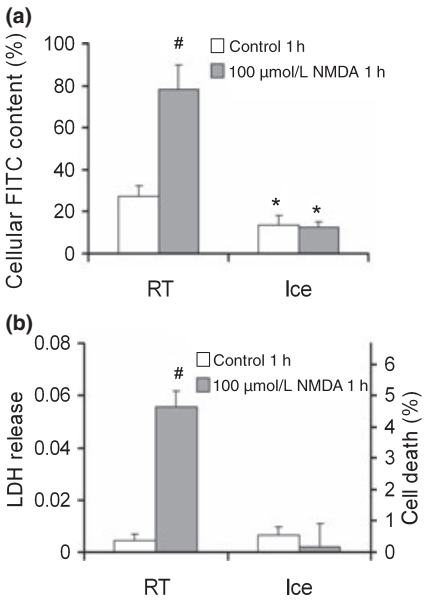

Fig. 2 Effect of lowering the temperature on *N*-methyl D-aspartate (NMDA)-induced endocytosis. Neurons were incubated on ice for 30 min before NMDA-administration and throughout the 1 h exposure, or for 90 min (control), or were maintained at 22°C (RT). (a) Uptake of 4.4-kDa fluorescein isothiocyanate (FITC)-dextran. ANOVA showed a significant difference between the four groups ($p < 0.0001$). Comparisons with RT groups: $*p < 0.05$ (*t*-test); effect of NMDA in RT group: $\#p = 0.016$ (*t*-test). (b) Lactate dehydrogenase (LDH) release in the same cultures. $n = 3$, ANOVA showed a significant difference between the four groups ($p < 0.0001$). Effect of NMDA in RT group: $\#p = 10^{-5}$ (*t*-test). Error bars represent SEM.

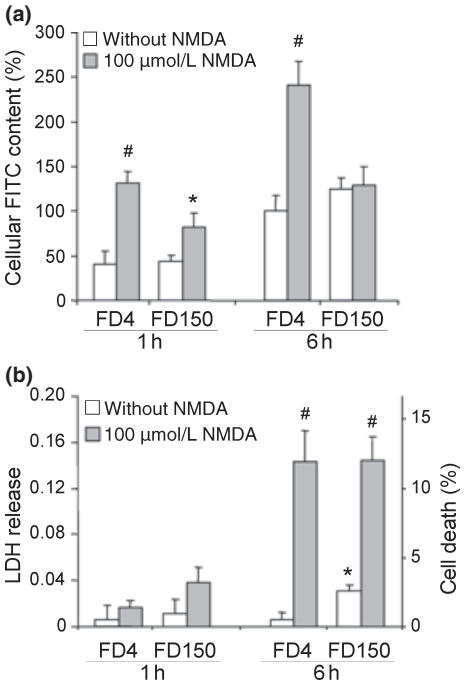

Fig. 3 (a) Size-dependence of fluorescein isothiocyanate (FITC)-dextran uptake following 100 µmol/L *N*-methyl D-aspartate (NMDA). Neurons were incubated with 0.5 mg/mL of two different sizes of FITC-dextran [4.4-kDa, 4.4 kDa FITC-dextran (FD4) or 150-kDa, 150 kDa FITC-dextran (FD150)] for either 1 or 6 h. Relative fluorescence between the two was measured after each experiment and normalized. ANOVA showed significant differences between the four 1 h groups ($p = 0.046$) and between the four 6 h groups ($p = 0.014$). Comparisons between corresponding NMDA and non-NMDA conditions: $*p < 0.05$, $\#p < 0.01$. (b) Lactate dehydrogenase (LDH) release, in the same cultures. The values have been normalized as in Fig. 1b. In the four 6 h groups, ANOVA indicated significant differences ($p = 0.0001$). Comparisons by *t*-test between corresponding NMDA and non-NMDA conditions: $\#p < 0.01$; between FD4 and FD150 at 6 h: $*p < 0.01$. Error bars represent SEM.

reduction, thus indicating a physiological, energy-dependent phenomenon, presumably endocytosis. The residual uptake, occurring even at 4°C was insensitive to NMDA (Fig. 2a). One hour exposure to 100 µmol/L NMDA at 37°C was only moderately toxic (0.5% cell death), and the incubation on ice protected totally against this; moreover, the 90 min incubation on ice was not itself toxic (Fig. 2b) although the cells could not resist ice treatment for several hours (not shown). Thus, both the constitutive and the NMDA-induced components of the FITC-dextran uptake were temperature dependent, indicative of a step requiring energy.

NMDA-induced endocytosis is size dependent

The size dependence of the endocytosis was evaluated using the small (4.4 kDa) FITC-dextran and a much larger one (150 kDa). As shown in Fig. 3, although the levels of constitutive endocytosis were comparable with the small and large dextrans, the NMDA-induced enhancement was minimal with the larger one, being weak at 1 h and non-existent at 6 h. This difference in size dependence suggests that the constitutive endocytosis is mainly due to macropinocytosis whereas the NMDA-induced component is mainly due to other mechanisms (see Discussion).

Neither component of the endocytosis is mediated by a receptor for dextran

To test if the endocytosis was receptor-mediated, we performed competition experiments using a 10 kDa non-fluorescent dextran (Figs 4a and b).The cells were incubated with unlabeled dextran at a concentration of 0.5 or 5 mg/mL for 10 min before addition of FITC-dextran (at 0.5 mg/mL). Neither in the presence nor in the absence of NMDA was FITC-dextran uptake significantly reduced by either dose of unlabeled dextran. These results indicate that neither the constitutive nor the NMDA-induced component of dextran uptake is receptor-mediated, at least not for dextran as ligand.

We then repeated the experiment of FITC-dextran uptake using free FITC (Fig. 4c). Uptake of free FITC was also enhanced in the presence of NMDA, raising the possibility that FITC might have served as a ligand for

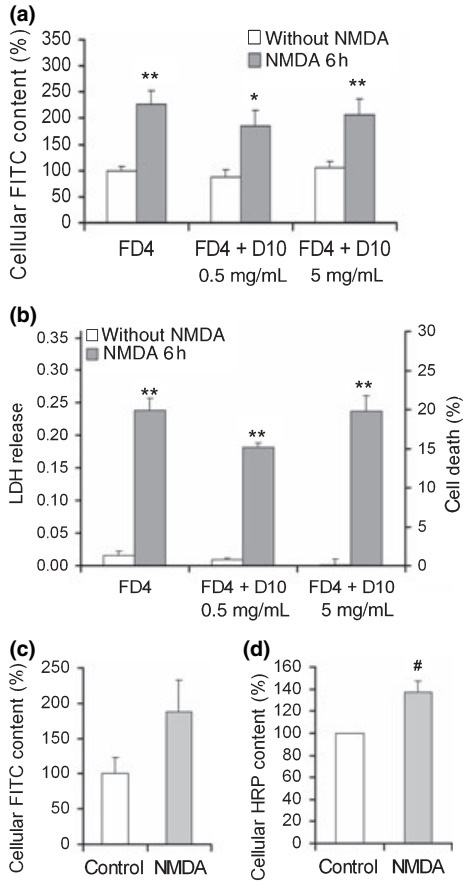

Fig. 4 Competition experiments with unlabeled dextran. (a) Uptake of 4.4-kDa fluorescein isothiocyanate (FITC)-dextran (FD4). Neurons were pre-incubated with 0.5- or 5-mg/mL 10-kDa unlabeled dextran (D10) for 10 min before exposure to 4.4-kDa FITC-dextran. ANOVA indicated significant differences between the six groups ($p = 0.0007$). Comparisons by *t*-test between corresponding *N*-methyl D-aspartate (NMDA) and non-NMDA conditions: $^{*}p < 0.05$, $^{**}p < 0.01$. (b) Lactate dehydrogenase (LDH) release, in the same cultures. The values have been normalized as in Fig. 1b, $n = 4$. ANOVA indicated significant differences between the six groups ($p = 0.0001$). Comparisons by *t*-test between corresponding NMDA and non-NMDA conditions: $^{**}p < 0.01$. (c and d) Uptake of two other ligands following NMDA exposure. Neurons were incubated with free FITC (1.25 μg/mL) or horseradish peroxidase (HRP, 0.5 mg/mL) for 6 h in presence or not of 100 μmol/L NMDA. $\#p < 0.01$ compared with non-NMDA control, *t*-test. Error bars represent SEM.

receptor-mediated. However, further experiments indicated that the uptake of HRP was also enhanced by 6 h of 100 μmol/L NMDA exposure (Fig. 4d). In view of the diversity of ligands endocytosed, and the lack of competition with unlabeled dextran, it would seem that the NMDA-induced endocytosis is not dependent on a specific receptor. The LDH assay confirmed that neither free FITC nor HRP were toxic or affected by the NMDA toxicity (results not shown).

The enhanced endocytosis of FITC-dextran depends mainly on NMDA-receptors

N-Methyl D-aspartate, KA, or GLU (100 μmol/L in each case) were applied in the presence or absence of the non-competitive NMDA antagonist MK-801 (40 μmol/L). The results in Fig. 5a show that each of these agonists was able to induce an enhanced uptake of 4.4 kDa FITC-dextran (FD4). NMDA-induced endocytosis was totally blocked by MK-801 (96% reduction of the induced component, $p \leq 10^{-4}$) and GLU-induced endocytosis was likewise strongly inhibited (by 85%, $p = 0.067$). KA-induced endocytosis was weaker, and was partially blocked by MK-801 (by 32%, $p \leq 0.05$). The strong inhibition of GLU-induced endocytosis by MK-801 suggests a predominant role of NMDA receptors in this phenomenon. MK-801 almost totally protected against the toxicity of NMDA and GLU, as measured by LDH release in the medium, but only slightly reduced (by 17%) the toxic effect of KA (Fig. 5b).

The NMDA-induced endocytosis is Ca^{2+}-dependent

The role of extracellular Ca^{2+} was investigated by pre-incubating the cells with the calcium chelator EGTA (5 mmol/L). This strongly reduced the NMDA-induced endocytosis of FD4 (Fig. 5c, FD4 uptake reduced by 82%, $p \leq 0.001$), and slightly reduced also the constitutive component of the endocytosis (by 34.6%, $p \leq 0.05$). NMDA induced toxicity was abolished by the EGTA (Fig. 5d).

Depolarization-induced endocytosis occurred late and involved NMDA receptors

Neurons were exposed to 100 μmol/L NMDA or 90 mmol/L KCl for either 6 or 12 h. In the latter case, FITC-dextran was added for the last 6 h only to exclude a degradation of this molecule as compared with the 6 h experiment. The level of NMDA-induced endocytosis was comparable after 6 or 12 h (Fig. 6a), whereas high potassium induced an enhanced uptake only after 12 h of incubation. Moreover, the latter effect was almost totally abolished by MK-801, indicating that it required the activation of NMDA receptors. NMDA-induced toxicity increased over time (Fig. 6b), as did KCl-induced toxicity. MK-801 had no effect on the KCl toxicity after 6 h of exposure, but did protect after 12 h (by 31.5%, $p \leq 0.05$). Thus, the effects of MK-801 on depolarization-induced endocytosis and cell death occurred late, between 6 and 12 h, presumably because of the accumulation of GLU in the medium following its depolarization-induced release.

NMDA-induced nuclear accumulation of FITC-dextran

Cortical neurons showed marked cellular uptake when exposed to FITC-dextran for 1 h or more. In control condition (without NMDA), most neurons displayed a faint punctate fluorescence pattern, the FITC labeling appeared to be restricted to the cytosol and to be in cytoplasmic organelles, presumably endosomes and perhaps lysosomes

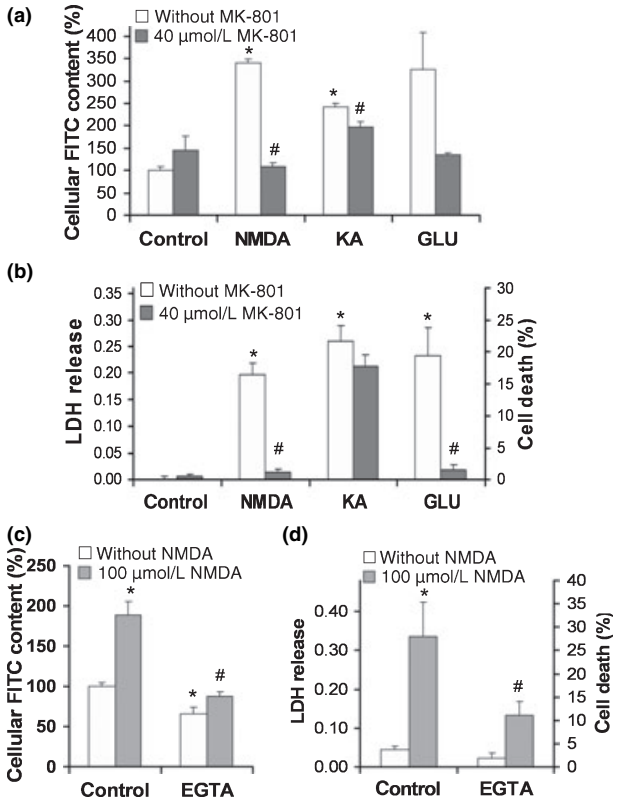

Fig. 5 Effects of different glutamate (GLU) agonists and of calcium on endocytosis and cell death. (a) Uptake of 4.4-kDa fluorescein isothiocyanate (FITC)-dextran after 6 h of either 100 μmol/L *N*-methyl D-aspartate (NMDA), 100 μmol/L kainate (KA), or 100 μmol/L GLU in the presence or absence of 40 μmol/L (5*S*,10*R*)-(-)-5-methyl-10, 11-dihydro-5H-dibenzo[a,d]cyclohepten-5,10-imine hydrogen maleate (MK-801) ($n = 3$). ANOVA showed highly significant differences between the eight groups ($p = 0.0001$). *t*-tests: $^*p \leq 10^{-4}$ in comparison with the non-agonist control without MK-801; $\#p \leq 0.05$ in comparison with the corresponding agonist-stimulated condition without MK-801. (b) Cell death in the same cultures, assessed from lactate dehydrogenase (LDH) release in the medium. ANOVA showed significant differences between the eight groups ($p \leq 0.0001$). *t*-tests: $p \leq 0.001$ in comparison with control (and without MK-801): $^*p \leq 0.001$ (*t*-test), $\#p \leq 0.001$ in comparison with the corresponding condition without MK-801. (c) Effect of the calcium chelator EGTA on 4.4-kDa FITC-dextran uptake ($n = 3$). 5 mmol/L EGTA was added to the medium 20 min before NMDA exposure. ANOVA showed highly significant differences between the four groups ($p = 0.0001$). *t*-tests: $^*p \leq 0.05$ in comparison with control without NMDA; $\#p \leq 0.001$ in comparison with NMDA-treated condition without EGTA. (d) Cell death measured in the same cultures. ANOVA showed significant differences between the four groups ($p = 0.0002$). *t*-tests: $^*p \leq 0.01$ in comparison with control; $\#p \leq 0.05$ in comparison with control conditions with or without NMDA-treatment. Error bars represent SEM.

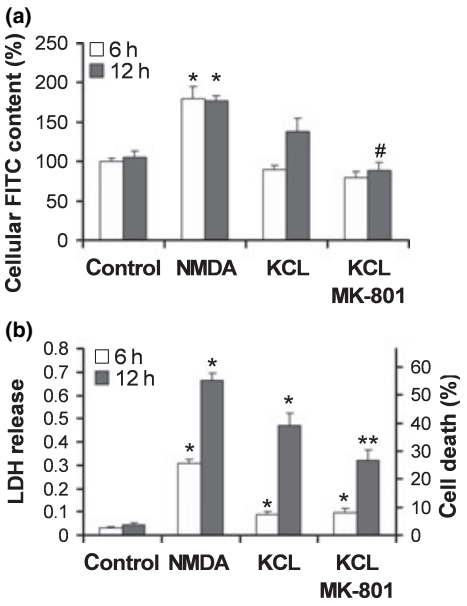

Fig. 6 Effects of *N*-methyl D-aspartate (NMDA) and of high potassium on endocytosis and cell death. (a) Uptake of 4.4-kDa fluorescein isothiocyanate (FITC)-dextran after 6 or 12 h of NMDA (100 μmol/L) or KCl (90 mmol/L) incubation. Neurons were pre-incubated for 10 min with 40 μmol/L (5*S*,10*R*)-(-)-5-methyl-10,11-dihydro-5H-dibenzo[a,d]cyclohepten-5,10-imine hydrogen maleate (MK-801) before KCl addition to the medium. FITC-dextran (0.5 mg/mL) was present in the medium for 6 h in both cases (for the last 6 h of incubation in the 12 h experiment). ANOVA showed highly significant differences between the eight groups ($p \leq 0.0001$). *t*-tests: $^*p \leq 0.01$ in comparison with the corresponding control; $\#p \leq 0.05$ in comparison with the 12 h KCl-treated condition without MK-801. (b) Cell death in the same cultures assessed from lactate dehydrogenase (LDH) released in the medium at the end of experiment. ANOVA showed highly significant differences between the eight groups ($p \leq 0.0001$). *t*-tests: $^*p \leq 0.01$ in comparison with the corresponding control; $\#p \leq 0.05$ in comparison with the 12 h KCl-treated condition without MK-801 or with the corresponding control. Error bars represent SEM.

(Fig. 7a). No cell death was detected by PI staining. Under 100 μmol/L NMDA treatment, FITC labeling was enhanced in the cytoplasm of neurons, but still more strikingly was very strong in neuronal nuclei (Fig. 7b). FITC staining of the nucleus was observed in 15.4% of cells after 1 h of NMDA and remained stable at 6 h of NMDA (12.7% of cells) (Fig 7c). Strikingly, none of the cells that displayed an enhanced fluorescence uptake were positive for PI staining, suggesting that the endocytic cells were not (yet) dying, and that dying neurons had ceased endocytosis (Fig. 7d).

Relationship between FITC-dextran endocytosis and cell death

As the neurons with strong nuclear FITC-dextran labeling in response to brief (1 or 6 h, Fig. 7c) NMDA exposure were unlabeled with PI, the question arises whether they die. We therefore tested the effects of longer exposure. Strikingly, after 24 h NMDA exposure, these neurons were no longer visible (Fig. 7, panel g_1). At this time-point, the cytoplasmic

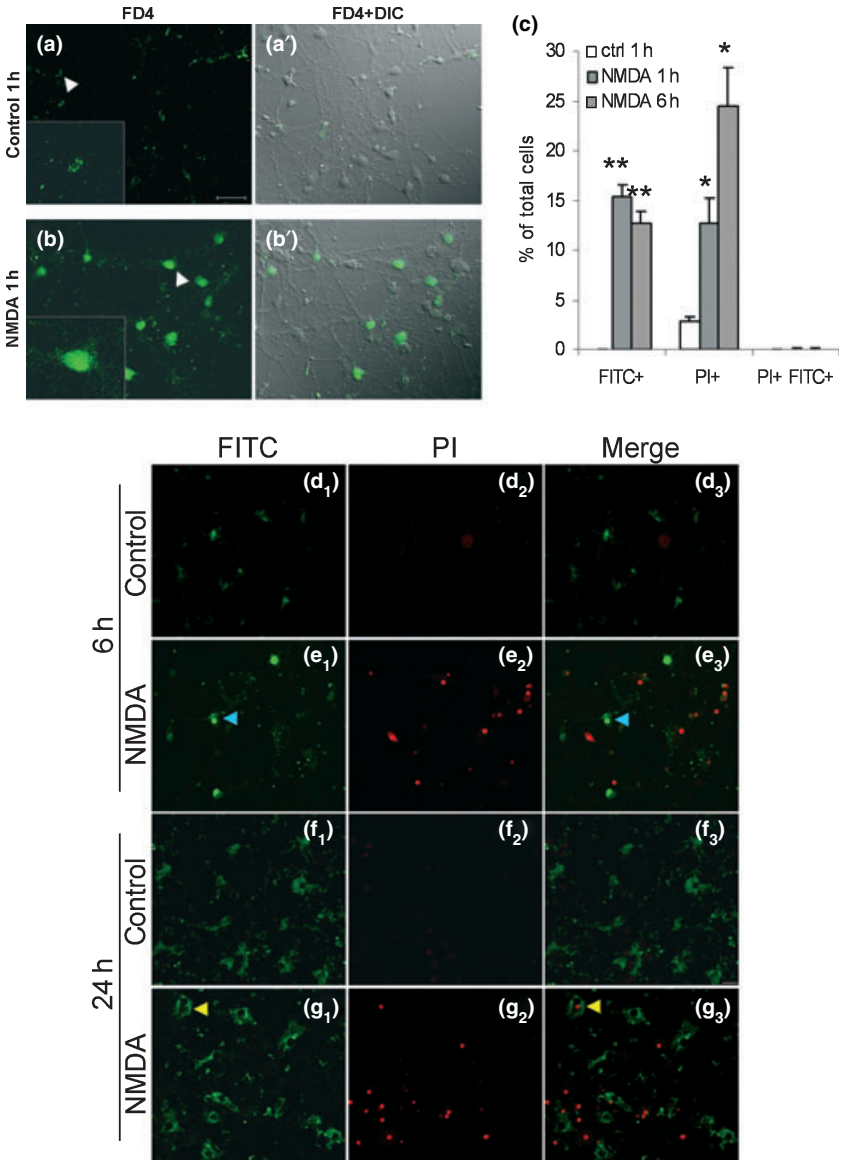

Fig. 7 Labeling with 4.4-kDa fluorescein isothiocyanate (FITC)-dextran (FD4) and propidium iodide (PI) after 1, 6, or 24 h exposure to *N*-methyl D-aspartate (NMDA), visualized by confocal microscopy. (a) Non-NMDA control condition after 1 h FITC-dextran exposure. (b) Effect of 1 h 100 μmol/L NMDA exposure on the FITC-dextran uptake. (a′ and b′) Combined fluorescence and differential interference contrast (DIC) imaging. Scale bar = 50 μm. Arrowheads indicate cells enlarged in insets. (c) Percentage of cells showing FITC labeling in the nucleus after 1 or 6 h exposure to NMDA and 4.4-kDa FITC-dextran, and percentage of PI labeled cells. Similar results were obtained with 6 h exposure to NMDA and FITC-dextran. Results are expressed as percentage of total cells as visualized by Dapi staining. $^{**}p < 10^{-6}$ compared with non-NMDA control; $^{*}p < 0.007$ compared with non-NMDA control (*t*-tests). (d) FITC-dextran exposure in control conditions for 6 h. (e) Effect of 100 μmol/L NMDA exposure for 6 h on FITC-dextran uptake (e_1) and cell death (e_2); e_3 shows combined fluorescence. Blue arrowhead shows a cell labeled with FD4 in the nucleus, but not with PI. (f) Neurons after 24 h of FITC-dextran exposure in control conditions. (g) Effect of 100 μmol/L NMDA exposure for 24 h on FITC-dextran uptake (g_1) and cell death (g_2); g_3 shows combined fluorescence. Yellow arrowhead shows a cell labeled with both FD4 (in cytoplasm) and PI. Scale bar, 20 μmol/L. Error bars represent SEM.

FITC-dextran labeling was much stronger than after 6 h of incubation and was comparable in the control and NMDA-treated condition (Fig. 7, panels f_1 and g_1), whereas after 6 h, the control labeling was still weak (panel d_1) and some neurons exposed to NMDA showed a strong FITC-dextran nuclear accumulation (panel e_1, blue arrowhead). In control conditions no or very rare neurons were labeled with PI (panels d_2 and f_2), whereas many were labeled following NMDA exposure, and their number increased between 6 and 24 h (panels e_2 and g_2). FITC-labeled nuclei did not contain PI after 6 or 24 h NMDA (panels e_3 and g_3), but after 24 h NMDA, many cells unlabeled with FITC or labeled only in their cytoplasm contained nuclear PI (panel g_3, yellow arrowhead).

Time-lapse experiments were performed to follow the fate of the neurons presenting a strong nuclear accumulation of dextran. AF488-dextran was used in these experiments because of its higher photostability as compared with FITC-dextran. Neurons displaying a nuclear accumulation of AF488-dextran appeared within 30 min. after NMDA exposure (Fig. 8), whereas control neurons displayed a punctate labeling in the cytoplasm. In the control condition, the level of fluorescence was comparable over 10:30 hours of experiment, indicating that the fluorophore did not bleach over this period of time and cells were still intact after 10:30 hours as shown by membrane integrity (yellow arrowhead). In the presence of NMDA, AF488-dextran labeling rapidly disappeared after 7:30 hours of incubation

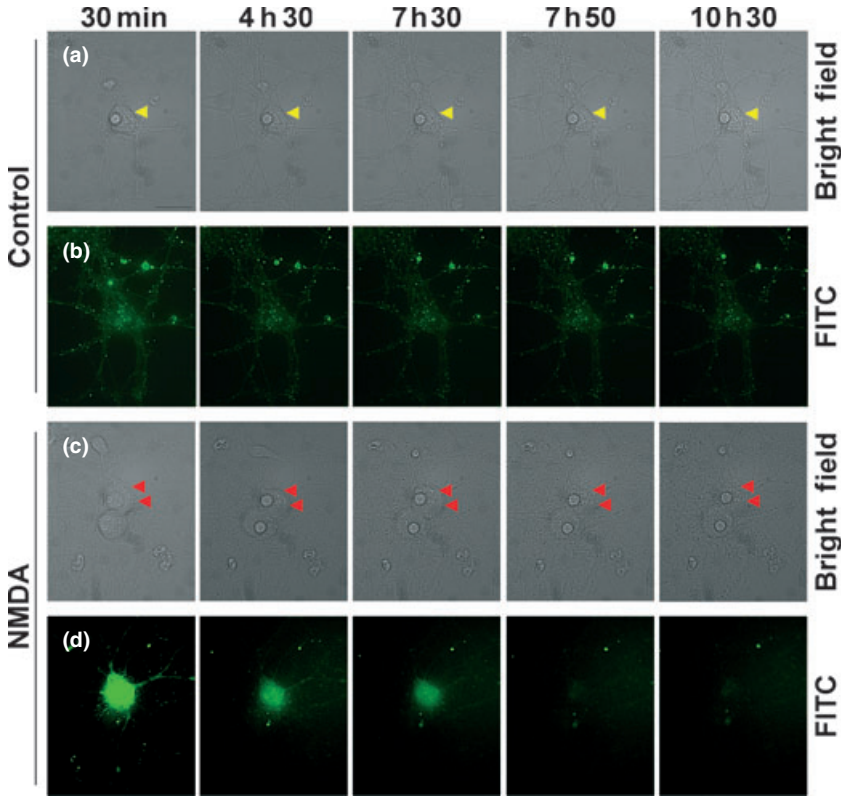

Fig. 8 Labeling with AlexaFluor 488 (AF488)-dextran over time. Shown are images of control or *N*-methyl D-aspartate (NMDA)-treated cells at 30 min, 4:30, 7:30, 7:50, and 10:30 hours after NMDA exposure. (a) Control condition, brightfield. Red arrowheads indicate cell membrane. (b) Control condition, fluorescence using fluorescein isothiocyanate (FITC) filters. (c) NMDA-treated condition, brightfield. (d) NMDA treated-condition, fluorescence for FITC. Scale bar = 20μmol/L.

and membrane integrity was impaired at the same time-point (red arrowheads).

JNK-dependence of the NMDA-induced component of endocytosis

We have tested the effects of D-JNKI1, a specific JNK inhibitory peptide. It totally blocked the NMDA-induced component of dextran endocytosis but had no effect on the constitutive component (Fig. 9b). By confocal microscopy, NMDA-exposed neurons pre-treated with D-JNKI1 (Fig. 9a) showed a distribution and intensity of FITC-labeling similar to that of the control without NMDA (Fig. 7a).

D-JNKI1 also almost totally inhibited the cell death induced by NMDA exposure, as shown by a complete loss of PI staining after 1 h (Fig. 9a) but also after 6 h (not shown) and a strong reduction in LDH release (85% reduction, Fig. 9c).

Discussion

The motivation for performing the present experiments was the observation of strongly enhanced endocytosis in retinal amacrine cells of chick embryos following intraocular injections of excitotoxic or near-excitotoxic doses of KA (Borsello *et al.* 2003a), and in organotypic hippocampal cultures following excitotoxic doses of NMDA (Borsello *et al.* 2003c). As a prelude to subsequent analysis of the signaling mechanisms underlying this phenomenon, we here establish nine main conclusions.

The NMDA-induced uptake of FITC-dextran (or free FITC or HRP) is by endocytosis

The fact that incubation of cells on ice eliminated the NMDA-induced FITC-dextran uptake as well as much of the constitutive component indicates that both components were due largely or entirely to endocytosis. Moreover, the alternative possibility of a passive entry of FITC-dextran following a membrane leakage in damaged neurons is excluded by the finding that the cells positive for FITC-dextran were negative for PI, and vice versa. This fits in with the published ultrastructural observation that the HRP taken into retinal amacrine cells following an intraocular injection of KA in chick embryos is located primarily in endosome-like organelles (Borsello *et al.* 2003a). Moreover, our ongoing experiments with pharmacological blockers of endocytosis confirm that both components are largely due to endocytosis.

Validity of the fluorescent assay

The above arguments for endocytosis confirm also the validity of the fluorescent assay. Conceivably, the assay could have been contaminated by the (perhaps transient) adherence of FITC-dextran to cell membranes. We attempted to eliminate these artifacts by multiple washing before

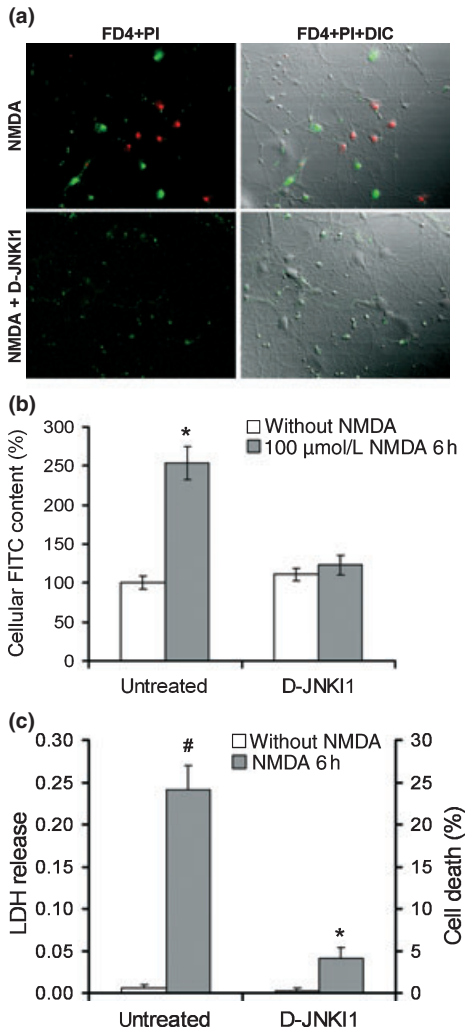

Fig. 9 c-*Jun* N-terminal protein kinase (JNK)-inhibition selectively eliminates the *N*-methyl D-aspartate (NMDA)-induced component of endocytosis and the neuronal death, 2 µmol/L D-JNKI1 was applied 1 h before NMDA exposure. (a) Visualization by confocal microscopy of labeling with 4.4-kDa fluorescein isothiocyanate (FITC)-dextran (FD4, green) and propidium iodide (PI, red). Neurons pre-treated with 2 µmol/L D-JNKI1 show labeling patterns similar to those of the controls (Fig. 5a). Scale bar = 50 µmol/L. (b) Quantification of FITC-dextran uptake, showing that the NMDA-induced uptake is blocked by D-JNKI1, $n = 9$ for all groups. $^*p < 10^{-4}$ with respect to each of the other groups (*t*-test). (c) Lactate dehydrogenase (LDH) release, in the same cultures, confirming the protection by D-JNKI1. $\#p < 10^{-5}$ with respect to non-NMDA untreated group. $^*p < 10^{-7}$ with respect to NMDA-exposed untreated group. Error bars represent SEM.

harvesting the cells, and by centrifugation to remove membrane fragments from the supernatant, whose fluorescence was measured. The small residual 'uptake' found even with incubation on ice may reflect contamination, or a minor component of uptake because of passive mechanisms, but as our main interest is in the NMDA-induced component of uptake, which was totally eliminated by incubation on ice, the assay is valid for our purposes. This assay is both quantitative and highly sensitive, and will therefore be valuable for further studies of this phenomenon.

The endocytosis involves two components with different characteristics

The fact that dextran size strongly affected the NMDA-induced component of cellular uptake, but not the constitutive component, indicates that different forms of endocytosis are involved in the two cases. Dextrans greater than about 10 kDa are taken up predominately by macropinocytosis, and 150 kDa dextran is specific for macropinocytosis (Araki *et al.* 1996). We found that 150-kDa FITC-dextran uptake was limited to the constitutive component of endocytosis, whereas 4.4-kDa FITC-dextran was in both, suggesting that the constitutive component is largely due to macropinocytosis, whereas the NMDA-induced component is of some other type (micropinocytosis, clathrin mediated endocytosis, etc.). The next step will be to determine which, using inhibitors of different types of endocytosis. A similar dependence on dextran size was found in chick embryo amacrine cells, where KA-induced endocytosis occurred with FD4, but not with 42 kDa FITC-dextran (Borsello *et al.* 2003a). The occurrence of excitotoxicity-related endocytosis of HRP in both the amacrine cell study and the present one may seem surprising in view of the relatively large molecular weight of HRP (44 kDa), but HRP molecules are essentially spherical and probably subject to much less steric hindrance than dextran (Matsukawa *et al.* 1997).

The induced endocytosis is mediated by calcium entry following the activation of NMDA receptors

The calcium chelator EGTA totally blocked NMDA-induced FD4 endocytosis demonstrating its dependence on calcium entry through NMDA receptors. Although other means of membrane depolarization such as incubation in high potassium or of excitotoxic stimuli such as GLU or KA can also trigger this endocytosis, they do so less strongly, and most of their effect appears to be due to the activation of NMDA-receptors by released GLU, as it is inhibited by the NMDA antagonist MK-801.

The NMDA-induced component occurs primarily in a subpopulation of neurons, in which the FITC-dextran is strikingly targeted to the nucleus

Microscopic counting indicates that approximately 15.4% of the cells show a strong nuclear FITC labeling. The number of FITC labeled neurons after 6 h of NMDA exposure is not significantly different from 1 h NMDA exposure, suggesting that this phenomenon occurs early after NMDA administration and concerns only a subpopulation of neurons. Time-lapse experiments also confirm the early occurrence of the phenomenon as it is detectable as soon as 30 min after

NMDA exposure. As measured by cellular FITC uptake, increasing the NMDA exposure triggers an enhancement of internalization, because of further accumulation of FITC-dextran in the same subpopulation of neurons. Identification of the highly endocytic subpopulation will be further examined, but previous studies showed a heterogenic response of intracellular Ca^{2+} to NMDA treatment in cortical cultures (Centeno *et al.* 2007), that suggests the existence of different neuronal subpopulations.

Neither component of endocytosis involves specific binding of the ligand to a saturable receptor

Competition with an unlabeled dextran had no effect on either component of FITC-dextran endocytosis. This suggests that neither component involved specific binding of the FITC-dextran to a saturable dextran receptor (such as the mannose receptor, which is expressed in cortical neurons (Burudi and Régnier-Vigouroux 2001) and can mediate the endocytosis of FITC-dextran (Hackstein *et al.* 2002). This does not rule out the possibility that the FITC part of the FITC-dextran contained a specific ligand, and free FITC was indeed internalized in both components of the endocytosis (although it may not have been free at the moment of endocytosis). However, the weight of evidence favors a non-specific uptake mechanism, as HRP was also taken up in the present study and in the previous amacrine cell study (Borsello *et al.* 2003a); and in organotypic hippocampal cultures HRP and microperoxidase were both taken up by NMDA-induced endocytosis (Borsello *et al.* 2003c). Moreover, apart from the size limitation with large dextrans, we have not found any molecule that is not taken up in excitotoxicity-associated endocytosis. The lack of ligand specificity argues against the need for a specific receptor.

Relation between the NMDA-induced endocytosis and neuronal death

The minimal dose for the NMDA-induced component to be detectable was about 30 μmol/L NMDA, which is close to the threshold for excitotoxicity in these cultures (about 30 μmol/L NMDA, Fig. 1b). Nevertheless, enhanced endocytosis could be detected using the fluorescent assay at a combination of dose and exposure time (30 μmol/L NMDA, 1 h exposure) that had not yet induced LDH release, and even with the strongly excitotoxic dose of 100 μmol/L NMDA, the neurons were intensely labeled with FITC dextran at a time when they showed no sign of cell death judged from PI staining. This is in harmony with previous results in chick embryo amacrine cells (Borsello *et al.* 2003a). Nevertheless, the neurons with nuclear FITC-dextran did ultimately die, as they were no longer present at 24 h of NMDA. Tracking of these neurons using time-lapse microscopy revealed the cell death dynamics. The fact that membrane disintegration was a rapid phenomenon accompanied by a total and rapid loss of intracellular fluorescence may explain why neurons were never stained with both FITC-dextran and PI.

The fact that the endocytosis occurs before cell death does not exclude its involvement in the death mechanism. Enhanced endocytosis has been associated with several cases of (non-excitotoxic) neuronal death (Clarke 1982; Hornung *et al.* 1989), and neurodegeneration (Cataldo *et al.* 1997), but in other cases of cell death it does not occur (Borsello *et al.* 2002), and in one case of apoptosis it was shown to be decreased below normal constitutive levels (Cosulich *et al.* 1997). In these cases the endocytosis was not shown to be causally implicated in the cell death, but in two studies of photoreceptor degeneration in mutant drosophila, the death mechanism was shown to be blocked by a dynamin mutation that blocked clathrin-dependent endocytosis (Alloway *et al.* 2000; Kiselev *et al.* 2000). And most relevant to the present study, NMDA-induced death of cultured hippocampal neurons was prevented by broad spectrum inhibitors of clathrin-mediated endocytosis or a specific inhibitor of α-amino-3-hydroxy-5-methylisoxazole-4-propionate receptor endocytosis (Wang *et al.* 2004).

The fact that excitotoxic treatment leads to enhanced endocytosis before the onset of cell death suggests that it may serve as a means for targeting drugs into excitotoxically stressed neurons before they die. We are currently exploring this, and have preliminary evidence that an equivalent endocytic phenomenon occurs in a clinically relevant model of cerebral ischemia (Vaslin *et al*. 2005).

Relevance of the present experimental model to the excitotoxicity-associated endocytosis described in intact tissues

If the present dissociated neuron model is to be used for clarifying the mechanisms of endocytosis induced by excitotoxic stimuli, it is important to be sure that the same phenomenon is occurring in the present model as in the previous studies in intact tissues: chick embryo amacrine cells (Borsello *et al.* 2003a) and hippocampal organotypic cultures (Borsello *et al.* 2003c). This criterion seems to be met, because the present NMDA-induced endocytosis has several striking points in common with the previous phenomena: both occur in viable neurons, but require a stimulus close to the excitotoxic threshold; both are inhibited by the JNK cascade inhibitor D-JNKI1 (see below); both lack ligand specificity; and both have a size limitation, occurring only with small dextrans.

Dependence of the NMDA-induced component of excitotoxicity on the JNK pathway

In many cases of excitotoxicity JNK is activated, and in the present model this occurs after as little as 10 min of NMDA treatment (Borsello *et al.* 2003b). Moreover, JNK inhibition has been shown in several cases to protect against excitotoxicity and cerebral ischemia (Borsello *et al.* 2003b;

Bogoyevitch *et al.* 2004; Guan *et al.* 2005), and in the present model, as the present experiments confirm, total protection is afforded by the retro-inverso peptide inhibitor D-JNKI1 (Borsello *et al.* 2003b). JNK is also causally implicated in several examples of endocytosis (Nakahara *et al.* 2004; Pelkmans *et al.* 2005), including NMDA-induced endocytosis (Borsello *et al.* 2003c). The relationship between signaling pathways mediating excitotoxicity and those mediating the associated endocytosis is largely unknown, but D-JNKI1 is known to block the excitotoxicity-induced activation of caspase-3 (Centeno *et al.* 2007), and caspases are known to modify endocytosis, which they can either increase (Sarin *et al.* 1998), or decrease (Cosulich *et al.* 1997).

Conclusion

Endocytosis induced by an excitotoxic stimulus may be important because of its possible implication in the mechanism of excitotoxicity, and because it provides a potential means for targeting drugs into the stressed cells. In the present paper, we show for the first time that dissociated cortical neuronal cultures reproduce the same phenomenon as in intact preparations and can therefore be used for analyzing it; we introduce a fluorescent assay to facilitate its quantitative analysis; and we characterize its basic properties, setting the stage for an in depth analysis.

Acknowledgements

We thank Vincent Mottier for technical assistance, Cécile Lebrand for help with the time-lapse experiments and comments on the manuscript, and Jean-Yves Chatton and Yannick Krempp of the Cellular Imaging Facility, University of Lausanne for experimental support. This research was supported by grants from the Swiss National Science Foundation (3100A0-101696) and from the European Community's Sixth Framework Programme to the Specific Targeted Research Project STRESSPROTECT (LHSM-CT-2004-005310).

References

Aarts M. M., Arundine M. and Tymianski M. (2003) Novel concepts in excitotoxic neurodegeneration after stroke. *Expert Rev. Mol. Med.* **2003**, 1–22.

Alloway P. G., Howard L. and Dolph P. J. (2000) The formation of stable rhodopsin–arrestin complexes induces apoptosis and photoreceptor cell degeneration. *Neuron* **28**, 129–138.

Araki N., Johnson M. T. and Swanson J. A. (1996) A role for phosphoinositide 3-kinase in the completion of macropinocytosis and phagocytosis by macrophages. *J. Cell Biol.* **135**, 1249–1260.

Arundine M. and Tymianski M. (2003) Molecular mechanisms of calcium-dependent neurodegeneration in excitotoxicity. *Cell Calcium* **34**, 325–337.

Bogoyevitch M. A., Boehm I., Oakley A., Ketterman A. J. and Barr R. K. (2004) Targeting the JNK MAPK cascade for inhibition: basic science and therapeutic potential. *Biochim. Biophys. Acta* **1697**, 89–101.

Bonny C., Borsello T. and Zine A. (2005) Targeting the JNK pathway as a therapeutic protective strategy for nervous system diseases. *Rev. Neurosci.* **16**, 57–67.

Borsello T., Mottier V., Castagné V. and Clarke P. G. H. (2002) Ultrastructure of retinal ganglion cell death after axotomy in chick embryos. *J. Comp. Neurol.* **453**, 361–371.

Borsello T., Bressoud R., Mottier V., Gonzalez N., Gomez G. and Clarke P. G. H. (2003a) Kainate-induced endocytosis in retinal amacrine cells. *J. Comp. Neurol.* **465**, 286–295.

Borsello T., Clarke P. G. H., Hirt L., Vercelli A., Repici M., Schorderet D. F., Bogousslavsky J. and Bonny C. (2003b) A peptide inhibitor of c-Jun N-terminal kinase protects against excitotoxicity and cerebral ischemia. *Nat. Med.* **9**, 1180–1186.

Borsello T., Croquelois K., Hornung J. P. and Clarke P. G. H. (2003c) N-methyl-D-aspartate-triggered neuronal death in organotypic hippocampal cultures is endocytic, autophagic and mediated by the c-Jun N-terminal kinase pathway. *Eur. J. Neurosci.* **18**, 473–485.

Burudi E. M. E. and Régnier-Vigouroux A. (2001) Regional and cellular expression of the mannose receptor in the post-natal developing mouse brain. *Cell Tissue Res.* **303**, 307–317.

Cataldo A. M., Barnett J. L., Pieroni C. and Nixon R. A. (1997) Increased neuronal endocytosis and protease delivery to early endosomes in sporadic Alzheimer's disease: neuropathologic evidence for a mechanism of increased beta-amyloidogenesis. *J. Neurosci.* **17**, 6142–6151.

Cavalli V., Vilbois F., Corti M., Marcote M. J., Tamura K., Karin M., Arkinstall S. and Gruenberg J. (2001) The stress-induced MAP kinase p38 regulates endocytic trafficking via the GDI:Rab5 complex. *Mol. Cell* **7**, 421–432.

Centeno C., Repici M., Chatton J. Y. *et al.* (2007) Role of the JNK pathway in NMDA-mediated excitotoxicity of cortical neurons. *Cell Death. Differ.* **14**, 240–253.

Clarke P. G. H. (1982) Labelling of dying neurones by peroxidase injected intravascularly in chick embryos. *Neurosci. Lett.* **30**, 223–228.

Conner S. D. and Schmid S. L. (2003) Regulated portals of entry into the cell. *Nature* **422**, 37–44.

Cosulich S. C., Horiuchi H., Zerial M., Clarke P. R. and Woodman P. G. (1997) Cleavage of rabaptin-5 blocks endosome fusion during apoptosis. *EMBO J.* **16**, 6182–6191.

Doble A. (1999) The role of excitotoxicity in neurodegenerative disease: implications for therapy. *Pharmacol. Ther.* **81**, 163–221.

Guan Q. H., Pei D. S., Zhang Q. G., Hao Z. B., Xu T. L. and Zhang G. Y. (2005) The neuroprotective action of SP600125, a new inhibitor of JNK, on transient brain ischemia/reperfusion-induced neuronal death in rat hippocampal CA1 via nuclear and non-nuclear pathways. *Brain Res.* **1035**, 51–59.

Hackstein H., Taner T., Logar A. J. and Thomson A. W. (2002) Rapamycin inhibits macropinocytosis and mannose receptor-mediated endocytosis by bone marrow-derived dendritic cells. *Blood* **100**, 1084–1087.

Hornung J. P., Koppel H. and Clarke P. G. H. (1989) Endocytosis and autophagy in dying neurons: an ultrastructural study in chick embryos. *J. Comp. Neurol.* **283**, 425–437.

Jarousse N. and Kelly R. B. (2001) Endocytotic mechanisms in synapses (Review). *Curr. Opin. Cell Biol.* **13**, 461–469.

Kirkham M. and Parton R. G. (2005) Clathrin-independent endocytosis: new insights into caveolae and non-caveolar lipid raft carriers. *Biochim. Biophys. Acta* **1745**, 273–286.

Kiselev A., Socolich M., Vinos J., Hardy R. W., Zuker C. S. and Ranganathan R. (2000) A molecular pathway for light-dependent photoreceptor apoptosis in *Drosophila*. *Neuron* **28**, 139–152.

Lebrand C., Dent E. W., Strasser G. A., Lanier L. M., Krause M., Svitkina T. M., Borisy G. G. and Gertler F. B. (2004) Critical role of Ena/VASP proteins for filopodia formation in neurons and in function downstream of netrin-1. *Neuron* **42**, 37–49.

Matsukawa Y., Lee V. H., Crandall E. D. and Kim K. J. (1997) Size-dependent dextran transport across rat alveolar epithelial cell monolayers. *J. Pharmaceut. Sci.* **86**, 305–309.

Nakahara T., Uchi H., Urabe K., Chen Q., Furue M. and Moroi Y. (2004) Role of c-Jun N-terminal kinase on lipopolysaccharide induced maturation of human monocyte-derived dendritic cells. *Int. Immunol.* **16**, 1701–1709.

Noraberg J., Kristensen B. W. and Zimmer J. (1999) Markers for neuronal degeneration in organotypic slice cultures. *Brain Res. Protoc.* **3**, 278–290.

Pelkmans L., Fava E., Grabner H., Hannus M., Habermann B., Krausz E. and Zerial M. (2005) Genome-wide analysis of human kinases in clathrin- and caveolae/raft-mediated endocytosis. *Nature* **436**, 78–86.

Richard J. P., Melikov K., Vives E., Ramos C., Verbeure B., Gait M. J., Chernomordik L. V. and Lebleu B. (2003) Cell-penetrating peptides. A reevaluation of the mechanism of cellular uptake. *J. Biol. Chem.* **278**, 585–590.

Sarin A., Haddad E. K. and Henkart P. A. (1998) Caspase dependence of target cell damage induced by cytotoxic lymphocytes. *J. Immunol.* **161**, 2810–2816.

Sorkin A. and von Zastrow M. (2002) Signal transduction and endocytosis: close encounters of many kinds. *Nat. Rev. Mol. Cell Biol.* **3**, 600–614.

Vaslin A., Puyal J., Waechter V., Borsello T. and Clarke P. G. H. (2005) Endocytosis and autophagy in cerebral ischemia and excitotoxicity. Abstracts of Brain'05, Amsterdam, 511.

Wang Y., Ju W., Liu L., Fam S., D'Souza S., Taghibiglou C., Salter M. and Wang Y. T. (2004) Alpha-amino-3-hydroxy-5-methylisoxazole-4-propionic acid subtype glutamate receptor (AMPAR) endocytosis is essential for N-methyl-D-aspartate-induced neuronal apoptosis. *J. Biol. Chem.* **279**, 41 267–41 270.

Waxman E. A. and Lynch D. R. (2005) N-Methyl-D-aspartate receptor subtype mediated bidirectional control of p38 mitogen-activated protein kinase. *J. Biol. Chem.* **280**, 29 322–29 333.

